IEEE Access
Multidisciplinary | Rapid Review | Open Access Journal

Received December 25, 2018, accepted January 16, 2019, date of publication January 31, 2019, date of current version February 20, 2019.

Digital Object Identifier 10.1109/ACCESS.2019.2895566

Neural Decoding of Synergy-Based Hand Movements Using Electroencephalography

DINGYI PEI, (Student Member, IEEE), VRAJESHRI PATEL, (Member, IEEE), MARTIN BURNS, (Student Member, IEEE), RAJARATHNAM CHANDRAMOULI, (Senior Member, IEEE), AND RAMANA VINJAMURI, (Senior Member, IEEE)

Sensorimotor Control Laboratory, Department of Biomedical Engineering, Stevens Institute of Technology, Hoboken, NJ 07030, USA

Corresponding author: Ramana Vinjamuri (ramana.vinjamuri@stevens.edu)

ABSTRACT The human central nervous system (CNS) effortlessly performs complex hand movements with the control and coordination of multiple degrees of freedom. It is hypothesized that the CNS might use kinematic synergies to reduce the complexity of movements, but how these kinematic synergies are encoded in the CNS remains unclear. In order to investigate the neural representations of kinematic synergies, scalp electroencephalographic (EEG) signals and hand kinematics were recorded from ten subjects during six representative types of hand grasping. Kinematic synergies were obtained from recorded hand kinematics using singular value decomposition. The recorded kinematics were then reconstructed using weighted linear combinations of synergies, and the optimal weights were computed using optimal linear estimation. Using EEG spectral powers as neural features, a multivariate linear regression model was trained on the weights of the kinematic synergies. Using this model, kinematics from the testing subset of data was decoded from the EEG features with threefold cross-validation. The results show that the weights of kinematic synergies used in a particular movement reconstruction were strongly correlated to EEG features obtained from that movement. EEG features were able to successfully decode synergy-based movements with an average decoding accuracy of 80.1 $\pm$ 6.1% (best up to 93.4 $\pm$ 2.3%). These results have promising applications in noninvasive neural control of synergy-based prostheses and exoskeletons.

INDEX TERMS Electroencephalography, principal component analysis, kinematic synergies, movement primitives, multivariate linear regression.

I. INTRODUCTION

Movement control involves coordination across multiple areas to integrate sensory and cognitive information, followed by motor planning and execution. The motor cortex is responsible for the majority of planning, executing, and controlling voluntary behavior and includes the premotor cortex, primary motor cortex, and supplementary motor area. Previous studies [1], [2] demonstrated that activity from those areas is related to movement generation including directional modulation, elbow/shoulder flexion/extension, and specific joint movement.

Producing movement in the upper limb involves coordinating more than 40 degrees of freedom (DoF) [3]. The brain could control each of these DoF individually, but this would result in highly complex control. In 1967, Bernstein [4] proposed the idea of synergy-based movement, which is based on two key concepts: 1) the central nervous system (CNS) adapts strategies that reduce the complexity of motor control and 2) the CNS may use global variables, instead of independent DoF, to reduce this complexity. Synergy control preserves the functional integrity of the collection of relatively independent DoF [5], providing a simplified, lower-dimensional space compared with controlling those DoF individually. By analyzing kinematics of hand joints only, it was found that the first principal component accounted for $\sim$70 to 95% of variance in hand grasping movements [6], [7]. Each of these patterns is considered a kinematic synergy. These kinematic synergies supported the major types of grasps that humans use.

As the CNS is a collection of networks that span multiple areas, an anatomical placement of hand synergies has not yet been defined. One of the challenges is determining the relationship between synergies and their underlying neural representations [8]. The multiple parallel interactions among motor areas may reflect dynamic functions of

The associate editor coordinating the review of this manuscript and approving it for publication was Mohammad Zia Ur Rahman.

hand movement. Within the primary cortex of monkeys, it has been shown that a 'hand' and 'arm' area exist and that selected neurons within these areas encode movement at multiple joints [9], [10]. Other neurons in this region are responsible for connecting the hand and arm regions [11]. Previous studies also demonstrated both single cell neural [12] and population activity of interneurons [13] are correlated with muscle synergies during hand movement in monkeys. Individual finger movements were also shown to be encoded by neurons in specific regions [14]. Specific hand grasp types, such as whole hand and precision [15], [16] have also been decoded from neural recordings. Some investigators have attempted to correlate neural activity with kinematic synergies. Saleh and colleagues [17] found high correlation between single unity activity and kinematic (postural) synergies in monkeys. These studies show that a hand-related spatial organization may exist within and/or across multiple motor-related areas. A temporal pattern, however, may be encoded through firing patterns, rather than distinct neuron populations. When Graziano *et al.* [18] stimulated neurons (500ms train) within the motor cortex, the movement of the hand to mouth was characterized by a bell-shaped velocity profile peaking at about 0.25ms into the stimulation. Functional magnetic resonance imaging (fMRI) [19], [20] and transcranial magnetic stimulation (TMS) [21] were used to find neural representations of hand synergies.

It is evident that multiple areas of the brain may be sources for synergy encoding or representation, while others may be responsible for synergy manipulation or control. Thus, this study is aimed to characterize various cortical brain regions in order to further the understanding of synergy control at the global cortical activity level using electroencephalography (EEG). EEG is one of the most widely used methods because of its greater applicability and sufficient temporal resolution. Previous studies have shown that motor execution can be represented in both low and high frequencies of cortical EEG. A majority of studies achieved hand movement profile reconstruction using low frequency EEG in the temporal domain [22]–[24], and amplitude modulations recorded from low-frequency bands can decode finger movement. Non-invasive EEG recordings have also been used to reconstruct time-series muscle activity [25]. EEG activities have been used to classify hand movement patterns [26] from delta band (0.2-4 Hz) and individual finger movements [27] from broad frequency range (>0.3 Hz) EEG activities.

In this study, scalp EEG signals were recorded during hand grasping. Six objects that span different grasp types were used, and grasp kinematics were recorded using CyberGlove. Kinematic synergies were determined from the recorded grasp postures and their reconstruction weights in these grasps were calculated. EEG features were then trained on kinematic synergy weights using multivariate linear regression. Using this model, kinematics was decoded from EEG with 3-fold cross validation. We then attempted to calculate the correlations between the reconstruction weights and EEG features and to localize the synergies to active regions in the motor cortex. Preliminary results from this study were published in [28].

II. MATERIAL AND METHODS

A. EXPERIMENTAL PARADIGM

Ten individuals (4 males, 6 females; mean age 23.0 ± 3.1 years) participated. All subjects are righthanded without any history of neurological abnormalities or disorders. As seen in Fig. 1A, each grasp task consisted of grasping an object placed 40 cm away from the midline of the subject's body. The hand starts in an initial resting position (20 cm to the right of the subject's midline), lasting 4 seconds. The subject then rapidly grasps the object after hearing an audio 'start' stimulus and holds the grasp until an audio 'stop' stimulus is heard (additional 4 seconds). The experimental timeline is provided in Fig.2. Subjects were asked to refrain from blinking or swallowing during the pre-stimulus resting portion and grasping portion, if possible. The six grasp tasks spanned different grip/grasp types found in activities of daily living (ADL). These objects were: screw driver (tripod), water bottle (cylindrical), CD (lateral), petri dish (spherical), handle (hook), and bracelet (precision). Each object was grasped with 30 repetitions, for a total of 180 grasping tasks per subject.

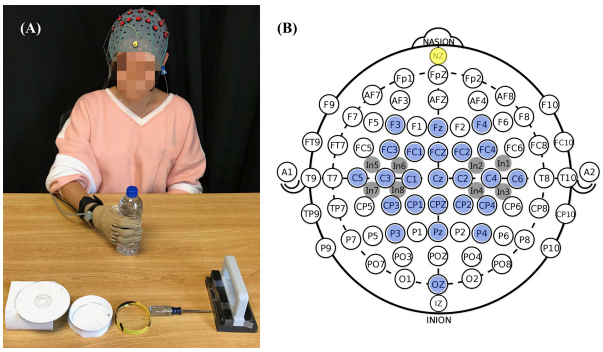

FIGURE 1. Experiment setup. Electroencephalography (EEG) and hand joint kinematics were recorded during grasping tasks. (A) For each task, the subject began in a flat palm resting position. After an audio stimulus, the subject rapidly grasped an object placed 40 cm away. The six objects used were screw driver, water bottle, CD, petri-dish, handle, and bracelet. (B) Neural signals were recorded from frontal, parietal, and occipital areas. 32 electrodes including 24 denominative channels (in blue) and 8 intermediate locations (in grey) were used.

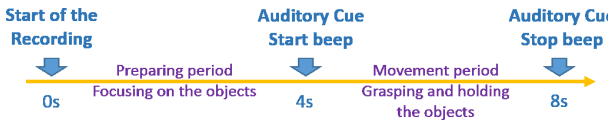

FIGURE 2. Experiment timeline. In the first 4 seconds, the subject focused on the object with the hand located in resting position. An audio 'start' stimulus was given at 4 seconds to indicate to the subject to grasp and hold the object until the 'stop' stimulus was heard.

B. DATA COLLECTION

Data was collected at Stevens Institute of Technology under an approved IRB protocol. A custom-built LabVIEW program provided the audio cues, collected CyberGlove data,

and sent a synchronizing wave to the amplifiers to align kinematic and EEG data. For neural signal acquisition, subjects wore a high-density EEG cap based on 10/20 system positions with an additional 86 intermediate positions (g.GAMMA cap, g.tec, Schiedlberg, Austria). During the experiment, EEG was recorded with 32 active electrodes. These electrode locations are: F3, Fz, F4, FC3, FC1, FCz, FC2, FC4, C5, C3, C1, CZ, C2, C4, C6, CP3, CP1, CPZ, CP2, CP4, P3, PZ, P4, OZ covering frontal (F), central (C), parietal (P) and occipital (O) areas. Eight other intermediate locations were also recorded (In1, In2, In3, In4, In5, In6, In7, In8, grey circles in Fig. 1(B)). A ground electrode was placed at the nasion (yellow) and reference (Ag, AgCl) electrode was on the right or left ear lobe. A conductive gel (g.GAMMAgel) was used to place each electrode (g.Ladybird). Impedance was kept below 5 kOhms and checked throughout the experiment. Data was continuously captured with two amplifiers (g.USBamp) using BCI2000 [29] with a sampling rate of 256 Hz. Kinematic data was recorded using a CyberGlove worn on the subjects' right hand. In this study, we used 10 of 18 sensors that measured the metacarpophalangeal (MCP) joints of the thumb and proximal interphalangeal (PIP) joints of the four fingers (IP for thumb). Each subject performed initial postures to calibrate the glove data. CyberGlove data was captured at 125 Hz using a custom-built LabVIEW (National Instruments Corporation, Austin, TX, USA) program.

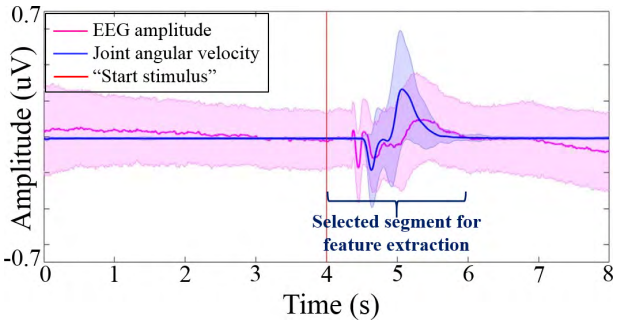

FIGURE 3. Recorded EEG and corresponding hand kinematics. EEG modulation (pink) is observed after the stimulus. Movement occurs almost at the same time in rapid grasp tasks. The PIP joint of the thumb (blue) is provided to show the alignment of EEG activity and movement. The shaded region indicated standard deviation.

C. EEG FEATURE EXTRACTION

EEG signals were first notch filtered at 60 Hz, followed by bandpass filtering in 1-45 Hz range. As shown in Fig. 3, EEG modulation is seen after the audio stimulus and movement occurs with a slight delay even in a rapid grasp task. Post-stimulus desynchronization is observed first, followed by post-stimulus synchronization, and then hand movement occurs. Neural activity gradually settles down accompanied with the end of movement 2 seconds post-stimulus. The hand grasp movement ends with an object holding phase. The time-varying band powers were calculated for 2 seconds from movement onset by a 750 ms wide sliding window with a 500 ms overlap. The band power within a window was calculated by averaging the energy, the sum of squared EEG potentials, as described in Equation 1.

$$P[n] = \frac{1}{N}\sum_{n=1}^{N} |x\,[n]\,|^2 \tag{1}$$

where P[n] and x[n] represent the average power and EEG amplitudes respectively. N is the number of samples within a time window. The 750 ms width was used to obtain a higher spatial resolution in the frequency domain. Since only 2 seconds were selected from stimulus onset to end of movement, 500 ms overlap was to ensure as much information as possible was included. A total of six features corresponding to six time periods were extracted for each electrode.

D. HAND KINEMATIC SYNERGIES

From a subset of grasp data, grasp kinematics were used to derive kinematic synergies. First, data from movement onset to movement completion was extracted from each grasp. As explained in [30], synergies were derived using singular value decomposition (SVD). With no time-delayed recruitments used for rapid grasps, the synergy model from [30] was reduced to:

$$v\,(t) = \sum_{p=1}^{P} c_p S_p \tag{2}$$

where $v(t)$ represents the angular velocity of joint at time t, c is the amplitude coefficient of synergy S, and P is the total number of synergies selected. The first three synergies are provided in Fig. 4. We used an 80% variance threshold to determine the number of synergies to be used in this decoder. Thus, we selected the first six synergies in the decoder with reconstruction error 0.1 (Fig. 5). Reconstruction (methods described in [30]) of the same subset data was performed to solve for vector C for each grasp.

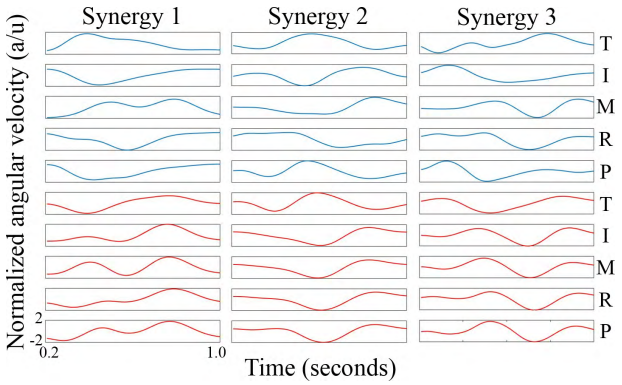

FIGURE 4. Joint Kinematics of three synergies. Normalized kinematic synergies derived from Subject 2 with MCP joint angular velocities (blue) and PIP joint angular velocities (red) are shown here.

E. CORTICAL CORRELATES OF KINEMATIC SYNERGIES

Previous studies [22], [24], [31] applied linear regression for modeling hand movements, where each joint movement is independently regarded as a linear combination of neural activities in time domain. In this paper, instead of joint movements, the weights of six synergies (response vectors)

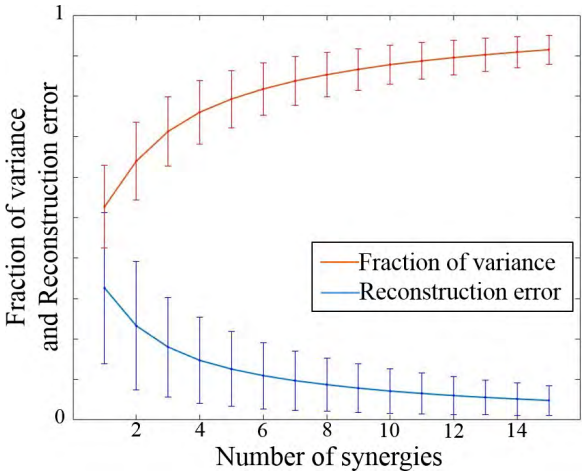

FIGURE 5. Fraction of variance and reconstruction error. Reconstruction error based on kinematic synergies decreases with the increase in the number of selected synergies. We selected the first six synergies with fraction of variance>80% and corresponding mean reconstruction error of 0.1 approximately.

are expressed by multiple neural features (variables). Thus, a multivariate linear regression model was used to determine the relationship between neural features and the weights of synergies:

$$C = X\beta \tag{3}$$

C represents the weights of synergies, determined by kinematic synergy-based reconstruction. For each task, C is a $n \times m$ matrix, where n is the number of repetitions and m is the number of synergy weights. X is a $n \times p$ neural feature matrix, and p represents the number of EEG features. The estimated regression parameter β was determined using the *mvregress* function in the Statistics and Machine Learning Toolbox in MATLAB. This function uses a maximum likelihood estimation to estimate, here, the diagonal elements of the variance-covariance matrix. β is a $p \times m$ coefficients matrix. This model was evaluated with 3-fold cross validation where two-thirds of repetitions (20 grasps) from each grasp type (a total of 120 grasps) was used for training β one-third of repetitions (10 grasps) from each grasp type (a total of 60 grasps) was used as the testing dataset to determine final decoding accuracy. Decoding accuracy between synergy reconstructed kinematics and neural decoded kinematics were measured using Pearson correlation coefficient (ρ). The decoding error is defined as 1-$|\rho|$. The decoding methodology is illustrated in Fig. 6.

In order to investigate how each synergy was modulated by brain activities in certain areas, we evaluated the independence of the EEG channels used for decoding by the following model:

$$D_{sn} = \sum_{k=1}^{K} \sqrt{\sum_{m=1}^{M} \beta_{mks}^2} \tag{4}$$

where D_{sn} represents n^{th} EEG channel for the s^{th} synergy. M is the number of regression parameters β calculated above, and K is the total number of grasping tasks.

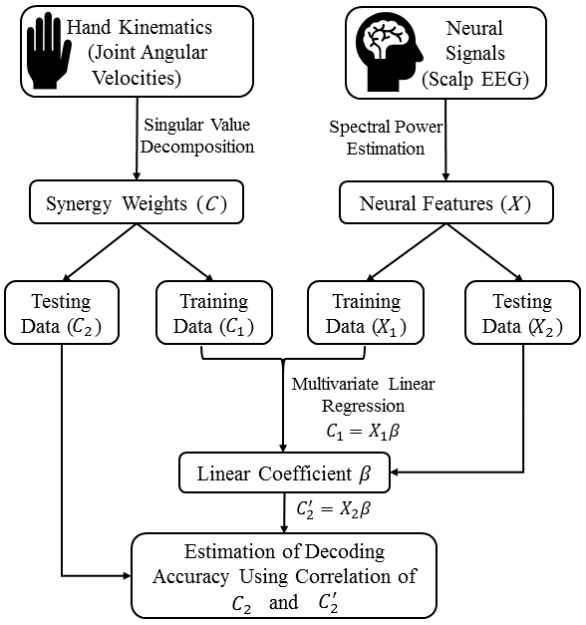

FIGURE 6. Decoding methodology. Weights of synergies obtained from SVD and neural features obtained from EEG signals are trained using multivariate linear regression. The linear coefficients obtained from training data were used to predict the synergy weights of the testing data.

III. RESULTS

Motor-related EEG activity is characterized by modulation of specific motor-related areas. EEG activity was averaged across all grasp types, repetitions, and subjects. Here the averaged activity of a wide frequency range 1-45Hz is shown in Fig. 7. Activity in the motor cortex increases post-stimulus and peaks during the movement. The supplementary motor area in the left hemisphere shows residual activation during the object holding phase. The correlation of synergies with EEG features was computed in order to find the cortical areas correlated with individual synergies. Fig.8 illustrates the correlation of synergies and EEG features. The first synergy and the sixth synergy are highly active in the beginning of the task (post-stimulus first phase of grasp) while the other synergies are activated later (grasp formation phase). It is observed that the synergies and EEG features are highly correlated during the action formation period. The correlation attenuated gradually when the grasp entered the hold phase. The synergies continued to remain mildly active in the left hemisphere in sensorimotor areas and parietal areas.

The average reconstruction accuracy rates achieved by neural decoding for all subjects are indicated in Table I. The averaged decoding accuracy rate across all subjects is 80.8±6.1% (best up to 93.4±2.3% for Subject 7). Averaged decoding errors based on joint types and grasp types are shown in Fig. 9. Based on neural decoding, for each joint (in blue) and for each grasp type (in green), it is shown that the MCP joints generally have lower error while the PIP joints of four fingers have relatively higher error. Tripod grasps (screw driver) had the highest error among all grasp types, while the cylindrical grasp (water bottle) observed lowest error.

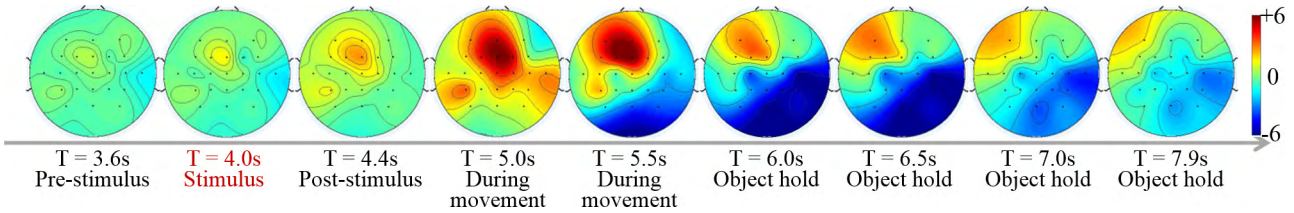

FIGURE 7. **Typical EEG activity during grasp. The averaged EEG activity amplitude from the wide frequency range of 1-45 Hz shows modulation in motor areas in all the tasks (color bar indicates the normalized amplitude of EEG activity). Activity in the motor cortex increases post-stimulus and peaks during the movement. The supplementary motor area in the left hemisphere shows residual activation during the object hold phase.**

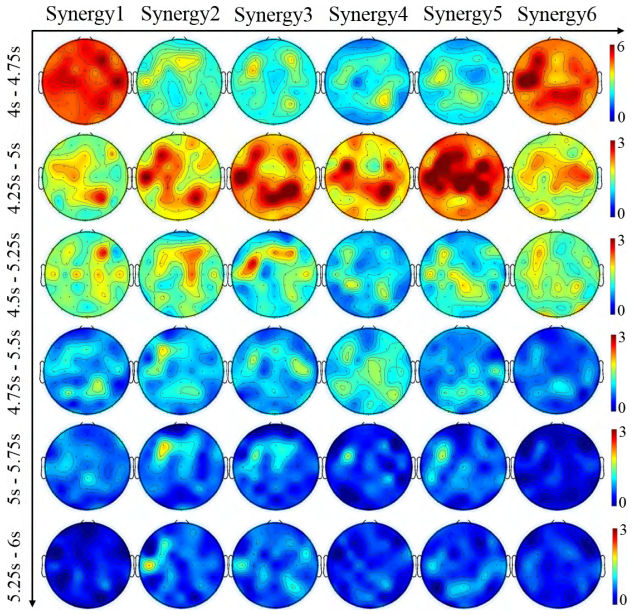

FIGURE 8. **Spatial correlation of synergies and each EEG features. The first six EEG features (band powers) corresponding to different times during a grasp are illustrated from top to bottom. Synergy modulation varies for each EEG feature. Synergies and EEG features are highly correlated in the action formation period. The correlation attenuates gradually from grasp to hold and later phases. Color bars indicate the correlation of synergies and EEG features.**

The trajectories of recorded kinematics, reconstructed kinematics based on kinematic synergies, and reconstructed kinematics based on neural decoding are provided in Fig. 10. Results showed that the model was able to decode the weights for different joint types and grasp types. Angular velocity trajectories were accurately reconstructed by the synergy-based neural decoding model. For simple grasps, such as grasping a water bottle or petri dish, decoded kinematics are close to recorded kinematics. For complex grasps, for example, precision grasp (Fig. 10(B)), the key digits involved were thumb, index and middle finger. The corresponding kinematics trajectories are predicted accurately, while the trajectories of ring and pinky finger varied slightly.

We evaluated the ability of the model to find the cortical areas correlated with kinematic synergies. It was observed that corresponding cortical areas for each synergy vary from subjects. Fig. 11 shows the synergy activated areas that were frequently shared among ten subjects. The electrodes which are highly correlated with synergies are located on bilateral hemispheres in the sensorimotor cortical areas.

IV. DISCUSSION

In this study, two models were used to decode the neural representations of synergy-based control mechanisms. First, kinematic synergy-based reconstruction of rapid grasp movement kinematics was used to determine the number of kinematic synergies as well as the weights of kinematic synergies for each grasp. The weights of each kinematic synergy were then linearly regressed with neural (EEG spectral power) features recorded during the corresponding movements. Decoding accuracies up to 95.6% were achieved, which holds promise for potential applications in noninvasive neural control of synergy-based prostheses and exoskeletons.

A. SYNERGIES SIMPLIFY COMPLEX CONTROL

In this study a synergy-based model was applied for reconstructing movement kinematics, calculating the individual contributions of synergies and their neural correlates to each grasp. The movements are characterized as weighted linear combinations of synergies, where each synergy is a coordinated movement pattern across several joints of the hand, expressed in joint angular velocities as shown in Fig. 4. In previously reported studies, individual finger movements (joint angular velocities) were decoded from nonhuman primates using the firing rates of neurons in primary motor cortex (M1) [32] and from human subjects [16], [23], [31] using intracranial EEG and scalp EEG.

Several studies achieved promising results in neural decoding of reaching and grasping movements. However, the complexity of the high dimensionality of joints and high DoF involved in movement control still needs further exploration. Some studies proposed simplified methods of recruiting hand movements with lower dimensional vectors. It is hypothesized that rather than directing individual DoF at each point in time, the CNS may work in a lower dimensional subspace [4], [33]–[35]. This hypothetical subspace is made of a minimal set of movement synergies, that have a ''spatial'' component describing coordination across multiple DoF as well as a ''temporal'' component describing coordination across time, which are generalizable across several movements. According to our model, the synergies can be expressed at the kinematic (joint) level but are controlled (spatially and temporally) at the neural level. Furthermore, it was observed that principal components extracted from TMS-induced finger movements resembled the end postures of synergies derived from voluntary movements [21].

TABLE 1. Neural decoding accuracies for all subjects.

Subject	1	2	3	4	5	6	7	8	9	10
Accuracy	73.9±4.4	85.0±6.8	72.0±4.4	69.0±6.9	71.2±6.3	89.9±3.1	93.4±2.3	85.3±4.3	82.3±11.4	68.6±11.8

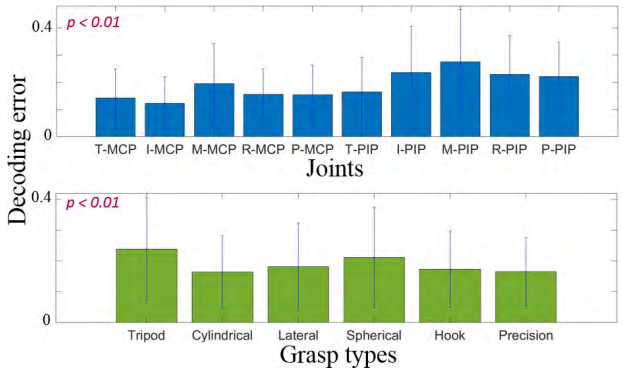

FIGURE 9. Decoding error based on joints (in blue) and grasp types (in green). MCP joints generally have lower errors while PIP joints have relatively higher error.

This experimental evidence further supports that the concept of synergies is not just theoretical but could be used as an optimal central mechanism for control by the CNS in simplifying and achieving complex movements.

B. NEURAL BASES OF HAND KINEMATICS AND SYNERGIES

Several model-free neural decoding and kinematic analysis findings have been reported in previous studies, nevertheless, our model-based approach led to successful decoding accuracies. Research in synergy-based models and models not based on synergies of hand movement showed that the brain regions unrelated to coordination are also active during synergistic movements [20]. Additionally, the ipsilateral hemisphere, dorsal premotor area and postcentral sulcus are highly active during the independent digit movements. Neural activities in bilateral motor areas are stronger in individuated movements than synergistic movements. Although we hypothesized that the hand grasp movement is composed of temporal postural synergies, individual digits still play an important role in achieving the movement. A simultaneous internal hierarchical model may be the reason behind the scalp EEG activities observed in the Figures 6, 7, and 10. In contrast to Fig. 6, which shows EEG activation in motor areas in contralateral hemisphere during hand movement, Fig. 7 and Fig. 10 show that the synergies were highly correlated with electrode activations in both hemispheres. Also, through the research on repetition suppression using fMRI, it was observed that there is a strong effect in the contralateral anterior intraparietal sulcus when the same object is grasped, and grasp trajectory is represented in the contralateral occipital sulcus and ipsilateral precentral sulcus [36].

Previous studies based on single unit recordings in nonhuman primates revealed that hand movement variables, such as hand velocity, and timing of execution of movements are encoded in the parietal cortices, cerebellum and frontal cortex [2], [37]. In agreement with these findings, our outcomes indicated that kinematic synergies were highly correlated with electrodes in parietal and frontal areas. Johnson-Frey *et al.* [38] pointed out that the inferior frontal regions are sensitive to detailed kinematic features when the hand and object have a functional relationship. In our experiment, the objects used were carefully chosen as representative grasps associated with the objects we commonly interact with in our activities of daily living. This further supports the results of this study as to why some synergies are active in bilateral hemispheres (Fig. 7 and Fig. 10).

C. DECODING HAND SYNERGIES USING EEG

Our previous studies on decoding asynchronous reaching directions [39] in arm movements and hand biometrics (extracting unique neural and behavioral movement markers) [40] from scalp EEG achieved promising outcomes, enabling us to probe further into decoding the functional details of hand movements in EEG.

In this study, we were able to demonstrate neural control of synergies to achieve hand grasps using multivariate regression. Very few studies have attempted to decode hand synergies during grasping in EEG. Agashe and Contreras-Vidal [22] used a regression analysis to model hand grasp using individual joint kinematics and low frequency (<1 Hz) EEG activity. They were able to achieve a correlation r- value of 76±1% between original and decoded grasps. Yoshimurae *et al.* [41] applied sparse logistic regression to decode finger movements using cortical current sources estimated from EEG, obtaining an average decoding accuracy of 72%. Acharya *et al.* [31] applied local motor potentials recorded using intracranial EEG to decode principal components of joint kinematics and achieved 51% accuracy. In our study, joint kinematic synergies were introduced, and weights of synergies were estimated using convex optimization and then regressed with cortical activities obtained from scalp EEG. We achieved an average decoding accuracy of 80.1±6.1% (best up to 93.4±2.3%).

In our study, EEG features extracted from power spectral densities (frequency range 1-45 Hz) were used to regress the weights of hand synergies utilized in grasping movement reconstruction. Previous studies have used slow cortical potentials (< 2 Hz) to decode hand and arm kinematics (velocity and position) via regression analysis [22], [23], [42]. Korik *et al.* [43] decoded movement kinematics from neural activities in the low delta band (0-2 Hz). Antelis *et al.* [24] pointed out that these studies may actually be overestimating decoding performance because of the natural relationship between slow cortical potentials and slow hand/arm

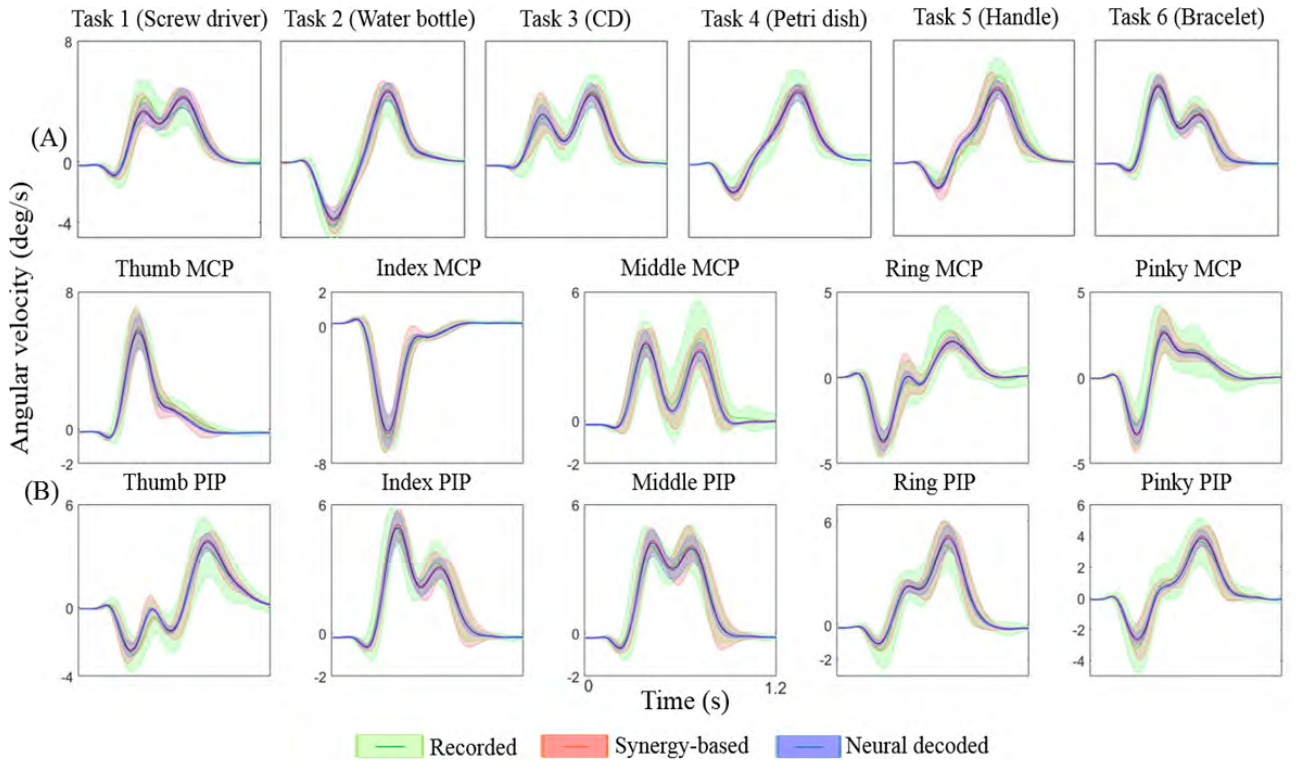

FIGURE 10. **Neural decoding of synergy-based movements. The recorded joint kinematics (green) were reconstructed by kinematic synergies (red) and neural decoded synergies (blue). The shaded regions show standard deviations. (A) Recorded and reconstructed joint angular velocities for index PIP joints in each grasp type for Subject 7. (B) Best reconstruction of joint angular velocities for each joint in Task 6 for Subject 7.**

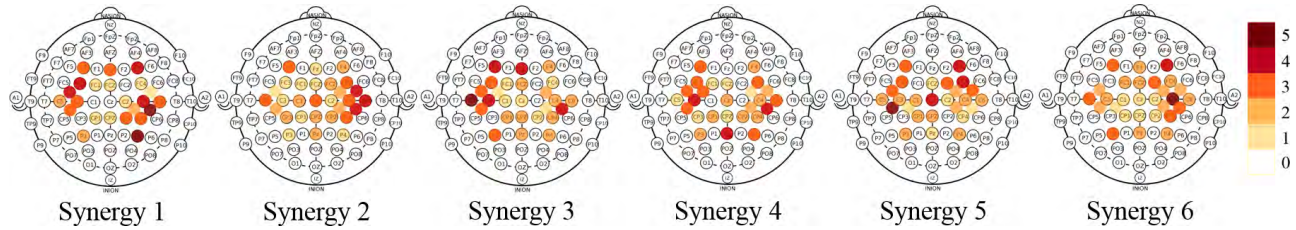

FIGURE 11. **EEG modulation for each synergy. Subjects have diverse cortical areas/electrodes corresponding to each synergy. The most commonly shared electrodes for synergies among ten subjects were ranked and selected for illustration. Top candidates are located in bilateral hemispheres around the sensorimotor cortex. The color bar indicates how often the electrodes were shared by synergies by the subjects.**

movements in time domain. However, this issue does not exist in the spatial domain of any frequency bands. Additionally, Korik *et al.* [43] pointed out that a band power based model provided a better performance in movement decoding. Therefore, our study was performed on rapid grasps decoded from EEG in the frequency domain (spectral powers in 1-45Hz frequency range) and not in lower frequencies, thus avoiding overestimation.

D. POTENTIAL APPLICATIONS OF SYNERGY-BASED MODELS IN NEURAL CONTROL OF PROSTHESIS

Reaching and grasping are the fundamental actions in interacting with the world around us. Unfortunately, this ability is lost in many individuals with motor disabilities. Currently, restoring lost limb functions are being demonstrated using innovative invasive and noninvasive brain machine interfaces [44]–[46]. Thus far, reliable neural control of ten-dimensional prosthetics was demonstrated successfully using highly invasive brain machine interfaces. Whether we can achieve high dimensional control using noninvasive technologies needs to be further explored. How to improve this control from 10 dimensions to the 25 dimensions present in natural human hand remains a challenge. In either modalities, synergy-based control [47] can help in expanding the application of limited and complex neural signals to control high dimensional end effectors.

V. CONCLUSION

In this study, we were able to decode neural correlates of kinematic synergies in rapid hand grasping movements in scalp EEG. We will consider the following aspects of improvement in the near future. The synergy-based movement generation model used in this study was simplified to weighted linear combinations of synchronous synergies

all combining at the same point in time. The model needs to be realized in its original asynchronous form allowing combination of synergies at different points in time. This increases the complexity of neural decoding. Furthermore, neural activities during motor planning occurring in premotor areas prior to movement execution were not considered in this study. Kawashima *et al.* [48] demonstrated that premotor and posterior parietal cortices generate neural activities during the planning phase, especially during the motor selection and choice reaction period. Additionally, in order to avoid any stimulus-related neural activations we may adapt asynchronous hand grasps that will involve self-selection of the tasks by the subjects. Finally, the relationship between neural features and kinematic synergies may be better estimated using nonlinear models than the model based on linear regression used in this study.

ACKNOWLEDGEMENT

The authors would like to thank the reviewers and editors for their valuable comments and critics that improved the quality of our manuscript significantly.

REFERENCES

[1] A. P. Georgopoulos, J. F. Kalaska, R. Caminiti, and J. T. Massey, "On the relations between the direction of two-dimensional arm movements and cell discharge in primate motor cortex," *J. Neurosci.*, vol. 2, no. 11, pp. 1527–1537, 1982.
[2] A. B. Schwartz and D. W. Moran, "Arm trajectory and representation of movement processing in motor cortical activity," *Eur. J. Neurosci.*, vol. 12, no. 6, pp. 1851–1856, 2000.
[3] C. L. Mackenzie and T. Iberall, *The Grasping Hand*, vol. 104, 1st ed. North Holland, The Netherlands: Elsevier, 1994.
[4] N. Bernstein, *The Co-ordination and Regulations of Movements*. Amsterdam, The Netherlands: Elsevier, 1966.
[5] M. T. Turvey, "Action and perception at the level of synergies," *Hum. Movement Sci.*, vol. 26, no. 4, pp. 657–697, Aug. 2007.
[6] P. Braido and X. Zhang, "Quantitative analysis of finger motion coordination in hand manipulative and gestic acts," *Hum. Movement Sci.*, vol. 22, no. 6, pp. 661–678, 2004.
[7] R. Vinjamuri, M. Sun, C.-C. Chang, H.-N. Lee, R. J. Sclabassi, and Z.-H. Mao, "Temporal postural synergies of the hand in rapid grasping tasks," *IEEE Trans. Inf. Technol. Biomed*, vol. 14, no. 4, pp. 986–994, Jul. 2010.
[8] M. C. Tresch and A. Jarc, "The case for and against muscle synergies," *Current Opinion Neurobiol.*, vol. 19, no. 6, pp. 601–607, 2009.
[9] H. C. Kwan, W. A. MacKay, J. T. Murphy, and Y. C. Wong, "Spatial organization of precentral cortex in awake primates. II. Motor outputs," *J. Neurophysiol.*, vol. 41, no. 5, pp. 1120–1131, 1978.
[10] B. J. McKiernan, J. K. Marcario, J. H. Karrer, and P. D. Cheney, "Corticomotoneuronal postspike effects in shoulder, elbow, wrist, digit, and intrinsic hand muscles during a reach and prehension task," *J. Neurophysiol.*, vol. 80, no. 4, pp. 1961–1980, 1998.
[11] M. C. Park, A. Belhaj-Saïf, M. Gordon, and P. D. Cheney, "Consistent features in the forelimb representation of primary motor cortex in rhesus macaques," *J. Neurophysiol.*, vol. 21, no. 8, pp. 2784–2792, 2001.
[12] S. A. Overduin, A. d'Avella, J. Roh, J. M. Carmena, and E. Bizzi, "Representation of muscle synergies in the primate brain," *J. Neurosci.*, vol. 35, no. 37, pp. 12615–12624, 2015.
[13] T. Takei, J. Confais, S. Tomatsu, T. Oya, and K. Seki, "Neural basis for hand muscle synergies in the primate spinal cord," *Proc. Nat. Acad. Sci. USA*, vol. 114, no. 32, pp. 8643–8648, 2017.
[14] R. Flamary and A. Rakotomamonjy, "Decoding finger movements from ECoG signals using switching linear models," *Frontiers Neurosci.*, vol. 6, p. 29, Mar. 2012.
[15] T. Pistohl, A. Schulze-Bonhage, A. Aertsen, C. Mehring, and T. Ball, "Decoding natural grasp types from human ECoG," *NeuroImage*, vol. 59, no. 1, pp. 248–260, 2012.
[16] J. Kubánek, K. J. Miller, J. G. Ojemann, J. R. Wolpaw, and G. Schalk, "Decoding flexion of individual fingers using electrocorticographic signals in humans," *J. Neural Eng.*, vol. 6, no. 6, 2013, Art. no. 066001.
[17] M. Saleh, K. Takahashi, and N. G. Hatsopoulos, "Encoding of coordinated reach and grasp trajectories in primary motor cortex," *J. Neurosci.*, vol. 32, no. 4, pp. 1220–1232, 2012.
[18] M. S. A. Graziano, C. S. R. Taylor, and T. Moore, "Complex movements evoked by microstimulation of precentral cortex," *Neuron*, vol. 34, no. 5, pp. 841–851, 2002.
[19] A. Leo *et al.*, "A synergy-based hand control is encoded in human motor cortical areas," *Elife*, vol. 5, Feb. 2016, Art. no. e13420.
[20] H. H. Ehrsson, J. P. Kuhtz-Buschbeck, and H. Forssberg, "Brain regions controlling nonsynergistic versus synergistic movement of the digits: A functional magnetic resonance imaging study," *J. Neurosci.*, vol. 22, no. 12, pp. 5074–5080, 2002.
[21] R. Gentner and J. Classen, "Modular organization of finger movements by the human central nervous system," *Neuron*, vol. 52, no. 4, pp. 731–742, 2006.
[22] H. A. Agashe and J. L. Contreras-Vidal, "Reconstructing Hand Kinematics During Reach to Grasp Movements from Electroencephalographic Signals," in *Proc. 33rd Annu. Int. Conf. IEEE Eng. Med. Biol. Soc. (EMBS)*, Aug./Sep. 2011, pp. 5444–5447.
[23] A. Y. Paek, H. A. Agashe, and J. L. Contreras-Vidal, "Decoding repetitive finger movements with brain activity acquired via non-invasive electroencephalography," *Front. Neuroeng.*, vol. 7, p. 3, Mar. 2014.
[24] J. M. Antelis, L. Montesano, A. Ramos-Murguialday, N. Birbaumer, and J. Minguez, "On the usage of linear regression models to reconstruct limb kinematics from low frequency EEG signals," *PLoS ONE*, vol. 8, no. 4, 2013, Art. no. e61976.
[25] N. Yoshimura, C. S. Dasalla, T. Hanakawa, M.-A. Sato, and Y. Koike, "Reconstruction of flexor and extensor muscle activities from electroencephalography cortical currents," *NeuroImage*, vol. 59, no. 2, pp. 1324–1337, 2012.
[26] J. G. Cruz-Garza, Z. R. Hernandez, S. Nepaul, K. K. Bradley, and J. L. Contreras-Vidal, "Neural decoding of expressive human movement from scalp electroencephalography (EEG)," *Frontiers Hum. Neurosci.*, vol. 8, p. 188, Apr. 2014.
[27] K. Liao, R. Xiao, J. Gonzalez, and L. Ding, "Decoding individual finger movements from one hand using human EEG signals," *PLoS ONE*, vol. 9, no. 1, 2014, Art. no. e85192.
[28] V. Patel, M. Burns, D. Pei, and R. Vinjamuri, "Decoding synergy-based hand movements using electroencephalography," in *Proc. 40th Annu. Int. Conf. IEEE Eng. Med. Biol. Soc. (EMBC)*, Jul. 2018, pp. 4816–4819.
[29] G. Schalk, D. J. McFarland, T. Hinterberger, N. Birbaumer, and J. R. Wolpaw, "BCI2000: A general-purpose brain-computer interface (BCI) system," *IEEE Trans. Biomed. Eng.*, vol. 51, no. 6, pp. 1034–1043, Jun. 2004.
[30] R. Vinjamuri, M. Sun, C.-C. Chang, H.-N. Lee, and R. J. Sclabassi, "Dimensionality reduction in control and coordination of the human hand," *IEEE Trans. Biomed. Eng.*, vol. 57, no. 2, pp. 284–295, Feb. 2010.
[31] S. Acharya, M. S. Fifer, H. L. Benz, N. E. Crone, and N. V. Thakor, "Electrocorticographic amplitude predicts finger positions during slow grasping motions of the hand," *J. Neural Eng.*, vol. 7, no. 4, 2010, Art. no. 046002.
[32] C. E. Vargas-Irwin, G. Shakhnarovich, P. Yadollahpour, J. M. K. Mislow, M. J. Black, and J. P. Donoghue, "Decoding complete reach and grasp actions from local primary motor cortex populations," *J. Neurosci.*, vol. 30, no. 29, pp. 9659–9669, 2010.
[33] M. C. Tresch, P. Saltiel, and E. Bizzi, "The construction of movement by the spinal cord," *Nature Neurosci.*, vol. 2, no. 2, pp. 162–167, 1999.
[34] M. Santello, G. Baud-Bovy, and H. Jörntell, "Neural bases of hand synergies," *Frontiers Comput. Neurosci.*, vol. 7, p. 23, Apr. 2013.
[35] M. Santello, M. Flanders, and J. F. Soechting, "Postural hand synergies for tool use," *J. Neurosci.*, vol. 18, no. 23, pp. 10105–10115, 1998.
[36] S. T. Grafton and A. F. de C. Hamilton, "Evidence for a distributed hierarchy of action representation in the brain," *Hum. Movement Sci.*, vol. 26, no. 4, pp. 590–616, 2007.
[37] D. W. Moran and A. B. Schwartz, "Motor cortical activity during drawing movements: Population representation during spiral tracing," *J. Neurophysiol.*, vol. 82, no. 5, pp. 2693–2704, 1999.
[38] S. H. Johnson-Frey, F. R. Maloof, R. Newman-Norlund, C. Farrer, S. Inati, and S. T. Grafton, "Actions or hand-object interactions? Human inferior frontal cortex and action observation," *Neuron*, vol. 39, no. 6, pp. 1053–1058, 2003.

[39] D. Pei, M. Burns, R. Chandramouli, and R. Vinjamuri, "Decoding asynchronous reaching in electroencephalography using stacked autoencoders," *IEEE Access*, vol. 6, pp. 52889–52898, 2018.
[40] V. Patel, M. Burns, R. Chandramouli, and R. Vinjamuri, "Biometrics based on hand synergies and their neural representations," *IEEE Access*, vol. 5, pp. 13422–13429, 2017.
[41] N. Yoshimura, H. Tsuda, T. Kawase, H. Kambara, and Y. Koike, "Decoding finger movement in humans using synergy of EEG cortical current signals," *Sci. Rep.*, vol. 7, no. 1, p. 11382, 2017.
[42] H. A. Agashe, A. Y. Paek, Y. Zhang, and J. L. Contreras-Vidal, "Global cortical activity predicts shape of hand during grasping," *Frontiers Neurosci.*, vol. 9, p. 121, Apr. 2015.
[43] A. Korik, R. Sosnik, N. Siddique, and D. Coyle, "Decoding imagined 3D hand movement trajectories from EEG: Evidence to support the use of mu, beta, and low gamma oscillations," *Front. Neurosci.*, vol. 12, p. 130, Mar. 2018.
[44] J. L. Collinger *et al.*, "High-performance neuroprosthetic control by an individual with tetraplegia," *Lancet*, vol. 381, no. 9866, pp. 557–564, Feb. 2013.
[45] S. Qiu, Z. Li, W. He, L. Zhang, C. Yang, and C.-Y. Su, "Brain–machine interface and visual compressive sensing-based teleoperation control of an exoskeleton robot," *IEEE Trans. Fuzzy Syst.*, vol. 25, no. 1, pp. 58–69, Feb. 2017.
[46] W. Wang *et al.*, "An electrocorticographic brain interface in an individual with tetraplegia," *PLoS ONE*, vol. 8, no. 2, 2013, Art. no. e55344.
[47] R. Vinjamuri *et al.*, "Toward synergy-based brain-machine interfaces," *IEEE Trans. Inf. Technol. Biomed.*, vol. 15, no. 5, pp. 726–736, Sep. 2011.
[48] T. Kawashima *et al.*, "Functional anatomy of GO/NO-GO discrimination and response selection—A PET study in man," *Brain Res.*, vol. 728, no. 1, pp. 79–89, 1996.

DINGYI PEI (S'18) received the B.S. degree in biomedical engineering from Tianjin University, China, in 2016, and the M.E. degree in biomedical engineering from the Stevens Institute of Technology, in 2018, where she is currently pursuing the Ph.D. degree in biomedical engineering. Her undergraduate and graduate research projects consisted of prosthetic control methods, brain–computer interfaces, biosignal detection circuit designs, and bio-signal and medical image processing. She received the Steven's Provost Doctoral Fellowship for current research. She also received the Third Prize in the International Contest of Applications in Nano-Micro Technologies, in 2014.

VRAJESHRI PATEL (M'13) received the B.S. and M.S. degrees in biomedical engineering from the New Jersey Institute of Technology, in 2011 and 2013, respectively, and the Ph.D. degree from the Department of Biomedical Engineering, Stevens Institute of Technology, in 2017. Her research interests include movement kinematics, prosthetic control methods, and quantification of neurodegenerative disease symptoms. She received the Steven's Innovation and Entrepreneurship Doctoral Fellowship for her work in biometrics.

MARTIN BURNS (S'17) received the B.S. degree in biomedical engineering and the M.E. degree in engineering management from the Stevens Institute of Technology, Hoboken, NJ, USA, in 2015, where he is currently pursuing the Ph.D. degree in biomedical engineering. His work was supported under the Innovation and Entrepreneurship Doctoral Fellowship. His research interests include robotics and control systems for assistive and rehabilitative robotics and brain–machine interfaces.

RAJARATHNAM CHANDRAMOULI (M'00–SM'06) was with the faculty of the Department of Electrical and Computer Engineering, Iowa State University, Ames. He is currently a Professor with the Department of Electrical and Computer Engineering, Stevens Institute of Technology, Hoboken, NJ, USA. His research interests include steganography, steganalysis, encryption, wireless networking, and applied probability theory. His research in these areas was sponsored by the National Science Foundation, the Air Force Research Laboratory, and industry. He was a recipient of the National Science Foundation CAREER Award. He was a Co-Founder and a Co-Program Chair of the IEEE International Workshop on Adaptive Wireless Networks in 2004 and 2005. He is also involved in several conference organizing committees. He has been an Associate Editor of the IEEE TRANSACTIONS ON CIRCUITS AND SYSTEMS FOR VIDEO TECHNOLOGY, since 2000.

RAMANA VINJAMURI (M'08–SM'11) received the B.S. degree in electrical engineering from Kakatiya University, India, in 2002, the M.S. degree in electrical engineering from Villanova University, Villanova, PA, USA, in 2004, and the Ph.D. degree in electrical engineering from the University of Pittsburgh, Pittsburgh, PA, USA, in 2008. He was a Research Associate with the Department of Physical Medicine and Rehabilitation, University of Pittsburgh, from 2008 to 2012. He was a Research Assistant Professor with the Department of Biomedical Engineering, Johns Hopkins University, from 2012 to 2013. He then joined the Department of Biomedical Engineering, Stevens Institute of Technology, as an Assistant Professor, in 2013. He is currently a Harvey N. Davis Distinguished Assistant Professor. His research was supported by the New Jersey Health Foundation and the Stevens Institute of Technology.